Tikrit Journal of Engineering Sciences (2022) 29 (4): 1-9
DOI: http://doi.org/10.25130/tjes.29.4.1

IRAQI Academic Scientific Journals

ISSN: 1813-162X (Print); 2312-7589 (Online)

Tikrit Journal of Engineering Sciences

available online at: http://www.tj-es.com

TJES Tikrit Journal of Engineering Sciences

College of Engineering

Theoretical Analysis and Development of an Artificial Neural Network Model to Evaluate Earthen Dam Slope Stability

*Ruqiya Abed Hussain, Asmaa Abdul Jabbar Jamel **

Civil Engineering Department, College of Engineering, Tikrit University, Tikrit, Iraq.

Keywords:

ANN; Core; Earth Dam; Horizontal Filter; Slope Stability

ARTICLE INFO

Article history:

Received	05 Sep. 2022
Accepted	23 Nov. 2022
Available online	05 Dec. 2022

Citation: Jamel AAJ, Hussain RA. Theoretical Analysis and Development of an Artificial Neural Network Model to Evaluate Earthen Dam Slope Stability. Tikrit Journal of Engineering Sciences 2022; 29(4): 1- 9.
http://doi.org/10.25130/tjes.29.4.1

ABSTRACT

In the design of earth dams, it must be considered that the water leakage through the earth dam generates upward and pore pressure, in addition to leakage forces that cause internal erosion, which has a direct influence on the structural stability of this system. Also, the rising and dropping in the water level has a direct effect on the stability of the dam's face slope. One way to solve these issues is the installation of a core or a horizontal water drainage system. The present study relied on the GEO-Studio computer tool to evaluate cross-sectional models of earthen dams by determining the safety factor under different situations represented by a change in filter type, and the flow state as a result of raising and lowering the water level at the dam reservoir and the full fill condition of the dam reservoir. The research found that the existence of a core substantially contributed to improving the safety coefficient for the case of rising the water level (2m) and rapidly rising by assigning it the greatest safety coefficient values. The absence of a filter had an opposite influence on the safety coefficient by decreasing it. Also, the factor of safety for the downstream slope was affected by less than 5% for different flow conditions, compared with the higher effect generated by the upstream slope. Furthermore, an artificial neural network model with an accuracy ratio of more than 97% was developed for the predicted safety factor.

* Corresponding author: E-mail: ms.asmaajameel@tu.edu.iq , Civil Engineering Department, College of Engineering, Tikrit University, Tikrit, Iraq.

التحليل النظري وتطوير نموذج الشبكة العصبية الاصطناعية لتقييم استقرار منحدر السد الترابي

رقية عبد حسين قسم الهندسة المدنية / كلية الهندسة / جامعة تكريت / تكريت - العراق.
اسماء عبد الجبار جميل قسم الهندسة المدنية / كلية الهندسة / جامعة تكريت / تكريت - العراق.

الخلاصة

عند تصميم السدود الترابية يجب الاخذ بنظر الاعتبار أن تسرب المياه خلال السد الترابي يولد ضغطا للإصعاد، اضافة الى قوى التسرب التي تسبب الانجراف الداخلي لتأثيرها المباشر على استقرار هذا المنشأ. كما ان الارتفاع والانخفاض بمنسوب الماء له تأثير مباشر على استقرار المنحدر الامامي للسد. ومحاوله للحد من هذه المشاكل فان استخدام لب مانع للتسرب أو استخدام منظومة تصريف مياه أفقية هو أحد الحلول. حيث اعتمدت الدراسة الحالية على استخدام البرنامج الحاسوبي GEO-Studio في تحليل نماذج مقطع السد الترابي لتقدير معامل الأمان ولحالات مختلفة متمثلة بتغير نوع المرشح المستخدم، وحالة الجريان نتيجة رفع وخفض منسوب الماء عند خزان السد وحالة ملئ خزان السد بالكامل. حيث أظهرت النتائج ان وجود اللب قد ساهم وبشكل كبير في تعزيز معامل الأمان في حالة ملئ خزان السد وحاله رفع السريع لمنسوب الماء وذلك بإعطائه اعلى قيم معامل امان. في حين ان عدم وجود مرشح كان له تأثير عكسي على معامل الأمان ليكون هو الأقل. أيضًا، تأثر عامل الأمان لمؤخر السد بقيمه أقل من 5٪ لظروف التدفق المختلفة، مقارنةً بتأثير اعلى ناتج عند ميلان مقدم السد. بالإضافة لذلك تم انشاء نموذج شبكة عصبية صناعية تعمل على التنبؤ بمعامل الأمان وبنسبة دقة اعلى من 97%.

الكلمات الدالة: ANN، اللب، سد ترابي، مرشح افقي، استقراريه المنحدر.

1. INTRODUCTION

Any soil structure with a slope is exposed to shear forces throughout the soil mass along the slope. It is related to gravitational effects attempting to draw down portions of the soil mass next to the slope. Various theories and analytical procedures, such as the technique of slices, were developed to estimate the critical slip surface and the associated safety factor, Eq.1: [1]

$$F.S = \frac{\tau_{Resisting}}{\tau_{\text{Mobilization}}} \quad \dots(\mathbf{1})$$

Also, the Artificial Neural Network (ANN) method has considerable potential in the technical monitoring of dams. This technique is conceptually and economically acceptable, as it avoids the need for difficult and costly unit replacement while still supplying information on the overall stability of the dam. Usama et al. [2] provided an analytical formula to compute the safety factor, which was dependent on the soil and hydraulic characteristics of the dam's shell, core, and filter. Using nine specified slope stability techniques, Spencer and General Limit Equilibrium (GLE) were the nearest to the safety conditions. Maimunah et al. [3] analyzed the effect of the reservoir water depth on the stability of non-homogenous earthen dam models. The lowest safety factor occurred at a slope of 1:1 with 1.4710. Also, the higher the water height, the more the slope deformed. Krikar et al. [4] investigated the effect of shell hydraulic conductivity on upstream slope stabilization during rapid drawdown. The most critical issue for the dam's upstream face with low hydraulic conductivity material is the water inside the soil slowly drains, which leads the dam's upstream slope to become unstable. Saleh et al. [5] investigated the probable slip surface of the zone earth dams with varying upstream heads under fast drawdown and earthquake activity. The upstream slope was found to be unstable during fast drawdown conditions with an earthquake-force impact of 0.1g, and the lowest value of the safety factor reported was 0.857. Hasan [6] compared the overall resistance and propelling forces used to calculate the safety factor against equilibrium loss. The computed amount of the safety factor was measured for the end stages, operating, and quick drawdown. Mohammed et al. [7] investigated Haditha dam and determined that the factor of safety readings for upstream and downstream slope safety matched the minimum standard for all water stages. Isaida et al. [8] evaluated the safety factor of the slope downstream using the Geo-Studio software for mattresses and flow spectra analysis. Higher slopes were achievable as a consequence of applying the rules of unsaturated soil mechanics considering the slope stability in earth dams. Abdolreza et al. [9] discovered that increasing the number of drains in the upstream shell of the upstream slope under sudden drawdown circumstances increased the stability factor. It was also discovered that constructing drains in the lower section of the upstream shell of earth dams provided better stability, than inserting drains at higher levels. Jelena et al. [10] designed a neural network model for predicting pore and total pressure in earth dams. As well, they demonstrated its operational use for finding complicated non-linear relationships between input and output parameters. Erzin et al. [11] created an Artificial Neural Network and Multiple Regression models to estimate the essential factor of the safety ratio of a standard natural slope exposed to seismic effects. Asmaa et al. [12] estimated the slope safety factor using an artificial neural network model coupled with the Geo-Studio

finding of a dam with a toe filter. The reported models had good accuracies (97.8% to 99.2%). Adnan et al. [13] checked the safety of the Shirin earthen dam at three different levels of the water reservoir. It was founded that the existence of the dam's core had a substantial influence on limiting the quantity of leakage through the dam's structure by (99%). Furthermore, it was discovered that the minimum safety factor was 1.95 and appeared around (4 days) of fast storage tank emptying, indicating that the upstream slope of the dams was stable throughout water removal. The rapid increase of water level always corresponds to the quick increase of hydraulic gradient and then a quicker seepage flow, which could further cause the instability of the earth's slope. The present study aims to estimate the safety coefficient of the dam's slope with various types of filters and for various flow cases involving rising, falling water levels, and rapidly rising and drawing down water in a reservoir. In addition, the present study aims to develop a neural network model that predicts the behavior of the dam's slope stability criteria.

2.SETUP METHODOLOGY

The present work was based on three earth dam models at unsteady flow. It was simulated using the Geo Studio program with various forms of filters (no filter, (model I); horizontal filter, (model II); and central core, (model III)), various upstream slopes $\frac{V}{H}\left(\frac{1}{3}, \frac{1}{2.25}, and\ \frac{1}{2.5}\right)$, and various values of the hydraulic conductivity coefficient (ky/kx) ratios (1, 0.5, and 2). While the unsteady flow was represented by rising and drawing down (2m) of the upstream head, and rapidly rising and drawing down the total upstream head in 7 days. Thus, 108 tests were performed, see Figs (1, 2, 3). For each test, the input and outcomes are stated in Eq. 2.

$$\begin{bmatrix} F.S\ for\ \frac{U}{S} \\ F.S\ for\ \frac{D}{S} \end{bmatrix} = f\left(\begin{matrix}\frac{\mathrm{U}}{\mathrm{S}}\ \mathrm{Slope}, \frac{ky}{kx}, \mathrm{Filter}, \mathrm{Flow\ case[Rise} \\ \mathrm{Up, Draw\ Down, Rapidly\ Rise\ Up,} \\ \mathrm{Rapidly\ draw\ down]}\end{matrix}\right) \ldots (2)$$

Figs (4, 5) show the critical slip surface, a factor of safety, and slip forces using the sub-programs SLOP/W.

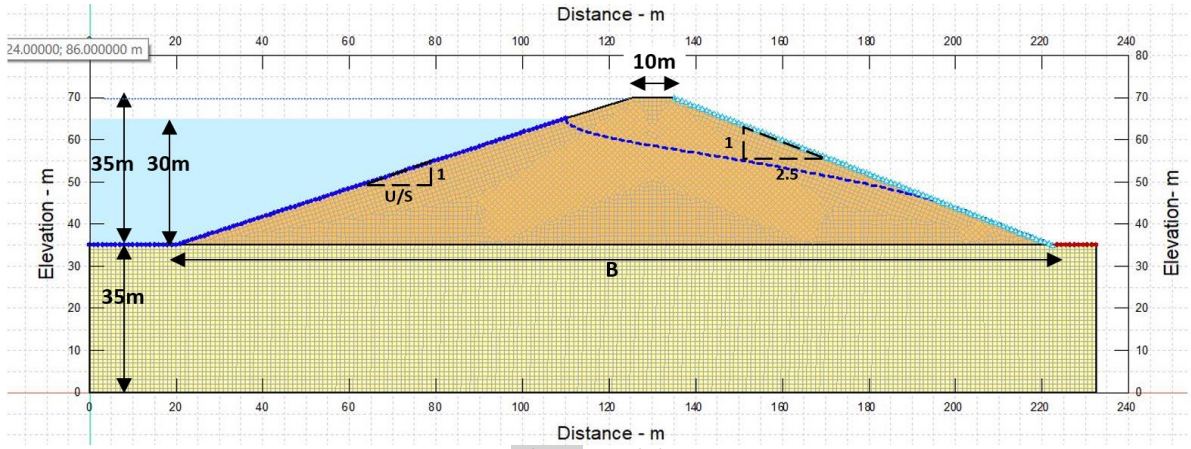

Fig 1. Model I.

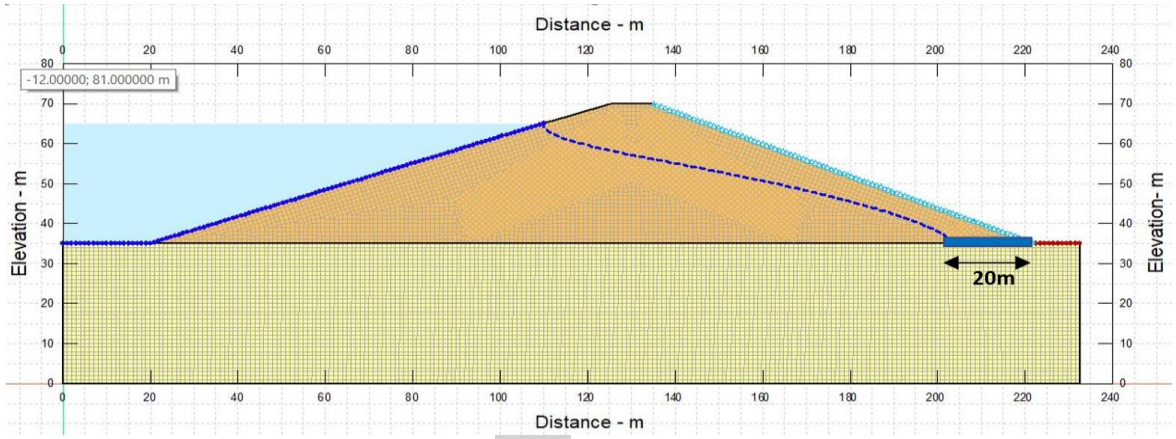

Fig 2. Model II.

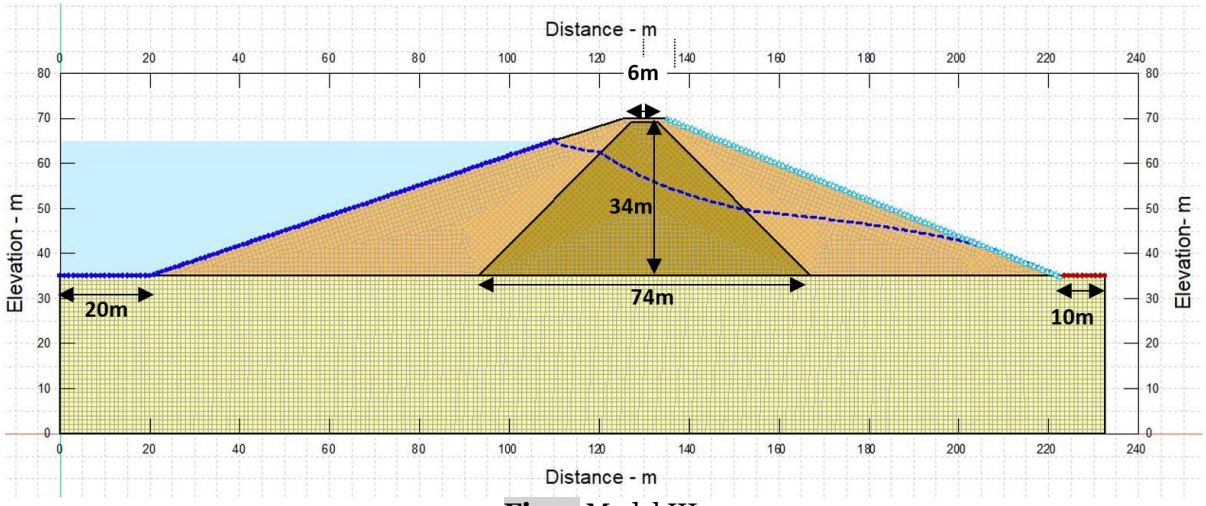

Fig 3. Model III.

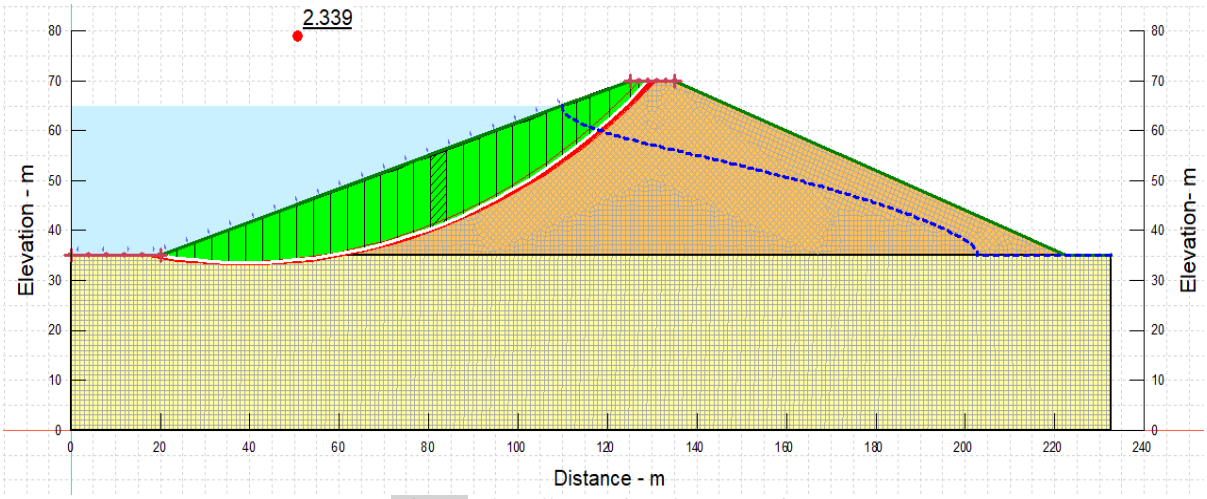

Fig 4. The Slip Surface by SLOP/W.

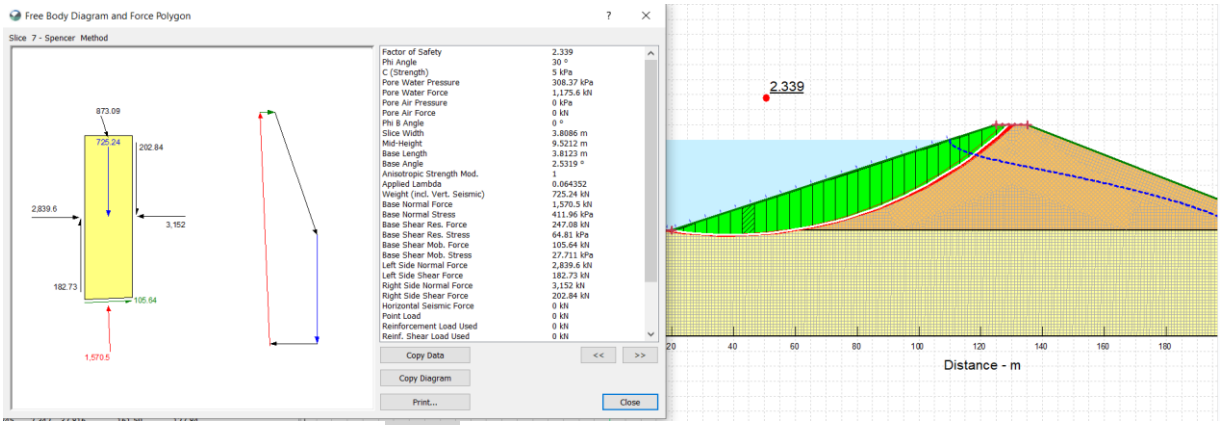

Fig 5. Slice Information by SLOP/W.

3.RESULTS AND DISCUSSION

3.1.Slope Stability at End of Construction and Steady State Flow

Table 1 shows the results of the safety coefficient in both the end of construction (case 1) and the end of filling the reservoir (case 2) cases, represented by the steady flow, the three models of dams, and both upstream and downstream of the dam. The results showed that the safety factor for all cases was higher than 1.5. Also, filling the reservoir contributed to increasing the safety factor of the upstream slope as the water in the reservoir stabilized the upstream slope. While a decrease in the safety coefficient of the downstream slope was observed as a result of filling the reservoir (constant flow condition).

Table 1. The factor of Safety ky/kx=1, U/S= 1:3

F.S		Model I	Model II	Model III
Upstream	Case 1	2.045	2.045	2.045
	Case 2	2.288	2.338	2.321

Downstream	**Case 1**	1.85	1.85	1.85
	Case 2	1.599	1.753	1.759

3.2.Slope Stability at Unsteady Flow

The results showed that the effect of a safety coefficient for the slope downstream of the dam, as a result of the rising and drawing down in water level at the dam's reservoir, differed in the safety coefficient from the condition of the steady state flow, with values below 5% for the first and second models, and less than 1% for the third model for various cases of flow condition, see Fig 8 Whereas the results showed a significant effect on the safety coefficient values of the upstream slope of the dam as a result of the change in the flow condition and for the studied models. The effect of the rising and drawdown of the water level had a significant impact on the upstream safety factor of the dam's upstream slope. For the three studied models, Fig 6 indicates the relationships between the permeability coefficient (ky/kx) and the upstream slope stability coefficient (F.S U/S) of the upstream dam, as a result of raising and reducing the water level and rapidly filling the dam reservoir. It is interesting to note that altering the permeability factor from (0.5) to (1) reduced the safety factor by (4.5%, 3.6%, 8.9%, and 1%) for model I, and each period of rising the water level, reducing the water, rapidly filling with water and rapidly draw down reservoir water, respectively. As these percentages are comparable for each of the three studied models in the present study. It is also valuable to note that the lowest value of the safety coefficient was for the case where the water level was lowered by (2m) and the permeability coefficient (2) was (2.176), whereas the lowest safety coefficient for the case that the water level (2m) raised and the permeability coefficient (2) was (2.302), which was higher than the previous case. The lowest result that was achieved while filling and drawing down the dam reservoir within seven days was with a permeability coefficient of (2) equals (2.95, and 1.593), respectively. It can be stated that the vertical permeability was greater than the horizontal permeability causing lower values of the safety coefficient. The presence of the core (model III) also considerably helped to improve the safety coefficient in the case of filling and drawing down rapidly the dam reservoir by giving it the greatest safety coefficient values. In addition, it showed the highest safety coefficient in the case of rising the water level. While model I caused the lowest values of safety factors for the four flow conditions (raising, lowering, emptying, and filling the reservoir). Fig 7 shows the upstream slope effect. It is noted that adapting the slope from (1:2.25) to (1:2.5) for a model I increased the safety coefficient by (7.8%, 8%, and 7.4%) for raising the water level (2m), lowering the water level (2m), and filling the dam's reservoir, respectively; besides reducing the safety coefficient by (1.7%) for rapidly drawing down the reservoir. It is also worth noting that the greatest value of the safety coefficient was (3.439) when the dam reservoir was filled in seven days, and the slope was steep (1:3). While rapidly drawing down in the dam reservoir had the lowest value (1.53) with (1:2.5). The difference in percentage between the previous two situations was (55.5%). So, it can be concluded that the condition of filling the dam reservoir within seven days posed insignificant danger compared to the drawn-down cases due to the large safety coefficient values.

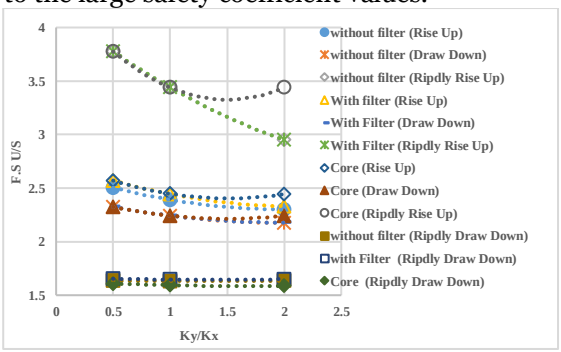

Fig 6. Relationship between the coefficient of permeability and factor of safety at U/S=1:3.

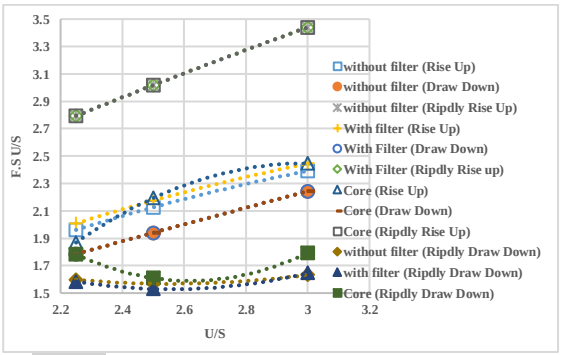

Fig 7. Relationship between the upstream slope and factor of safety at ky/kx=1.

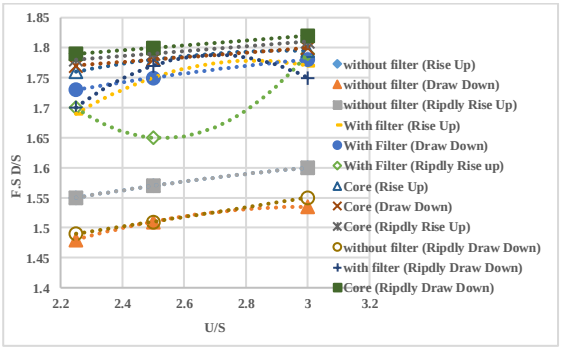

Fig 8. Relationship between the downstream slope and factor of safety at ky/kx=1.

Fig 9 indicates the change in the safety factor of the upstream dam's face with time., It was observed that when the water level raised, there was a quick increase in the safety factor, followed by a minor drop, until stabilizing at a

horizontal level. The initial rise in safety factor was because the water formed a vertical pressure that stabilized and strengthened the stability of the dam's front slope. Such behavior was opposite to what occurred when the water level was lowered or drawn down rapidly, where a quick decrease in the critical safety coefficient was noticed over time, followed by a steep rise in the safety coefficient's value. However, when the dam reservoir was filled, the safety coefficient was raised with a behavior similar to the rise in the water level. While Fig 10 shows a very low change in the downstream stability factor.

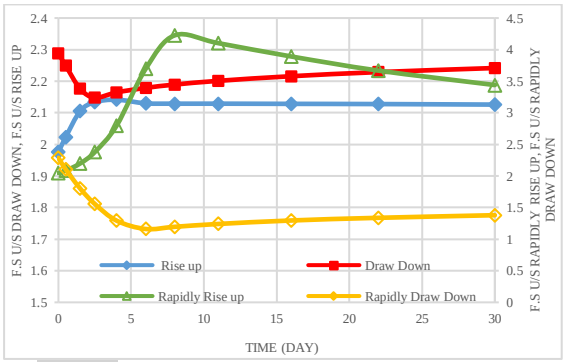

Fig 9. The change in the Upstream safety factor over time for model I.

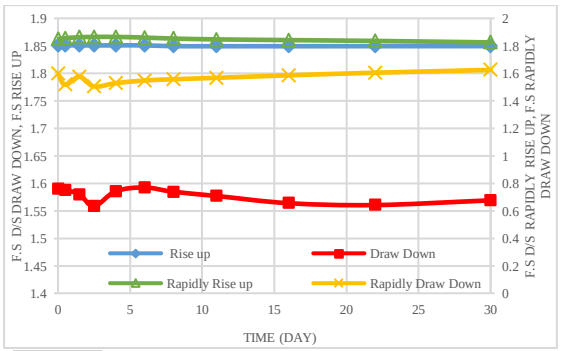

Fig 10. The change in the Downstream safety factor over time for model I.

Fig 11 (a) represents the slip shear resistance and shear mobilized below the slices of the critical slip surfaces for initial states and after the 7-day rise, which had identical values for the three models, to describe the behavior of the analyzed situation by its shell throughout the rapid rise up. The shear resistance was considerably larger than the shear mobilized in the initial state. From the beginning of the rising process until the end, the variation between shear mobilized and shear resistance tended to decrease, however, the shear mobilized was never greater than the shear resistance, indicating that the model was safe under fast rising. After the reservoir was filled, a difference in stress values between the three models began to form. After 60 days, there was a significant difference, as shown in Fig 9(b). The ultimate factor of safety was calculated by dividing the area below the resistance curve by the area below the mobilized shear curve.

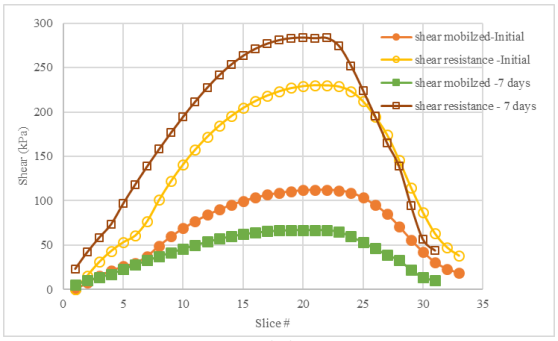

(a)

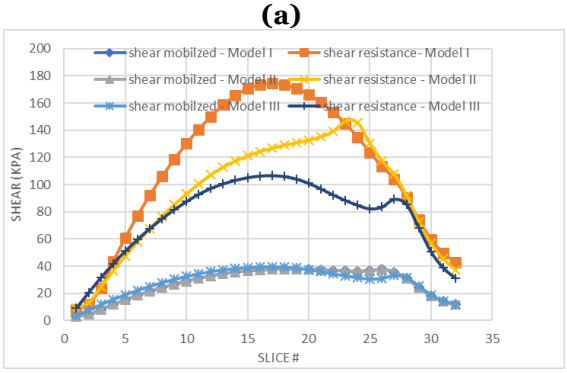

(b)

Fig 11. Slip shear mobilization and resistance at critical slip surface slices for rapid rise up at **(a)** initial condition, and 7 days, **(b)** 60 days.

3.3.ANN Models Results

Artificial neural networks (ANN) are equivalent to the human nervous system. The back-propagation network is the most commonly utilized form of neural network. The three-layer back-propagation network model has been proven to produce acceptable results for prediction and simulation in any engineering application [14]. The back-propagation method of the multilayer perceptron (MLP) was used in the present study, as shown in Fig 12. The back-propagation approach was based on the error correction learning function, which had two primary pathways. The input variable was applied to the network in the forward pathway, and its effects were transmitted via intermediate hidden layers to the output layer, where the output vector created the network's reasonable solution. The neural network structure comprised three levels: input, hidden, and MLP output layers, with several neurons evaluated for network layout in each layer. The number of available neurons in the input and output layers was determined by the nature of the issue under examination, whereas the number of neurons in the hidden layers, as well as the number of these layers, was decided by trial and error to decrease order and subsequently to decrease the model's percentage of error. In the present study, neural networks with two input nodes and three output nodes were studied in SPSS. The data were standardized using Eq. 3 depending on the output transfer function [14].

$$X_n = \frac{2(X-X_{min})}{X_{Max}-X_{min}} - 1 \quad \text{... (3)}$$

Table. 2 shows the estimated weight parameters, which were generated for the hidden and output layers' transfer functions (tangent hyperbolic-tangent hyperbolic). The input and output layers were divided into three groups: 70% for training, 10% to check that the network was generalizing and to terminate training before errors, and 20% to test the development due accurately independently. To obtain the results for the advanced models, the following expression, Eq. 4, was used.

$$\text{Output} = \sum_{j=1}^{n}(W_j * (\tanh(\sum_{i=1}^{m}(W_{ij} * (\text{Input})_i) + \text{Bias}_j))) + \text{Bias} \quad \ldots \textbf{(4)}$$

The accuracy of the results obtained based on the weights of the artificial neural network and the results obtained by Slope/W for models are shown in Figs (13, 14, 15).

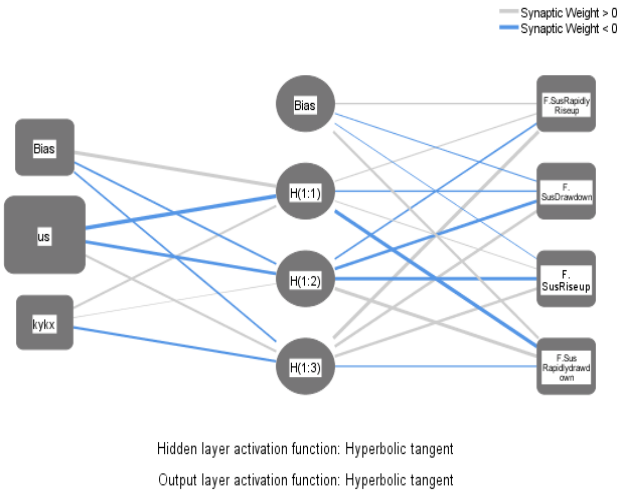

Fig 12. Artificial Neural Network Model.

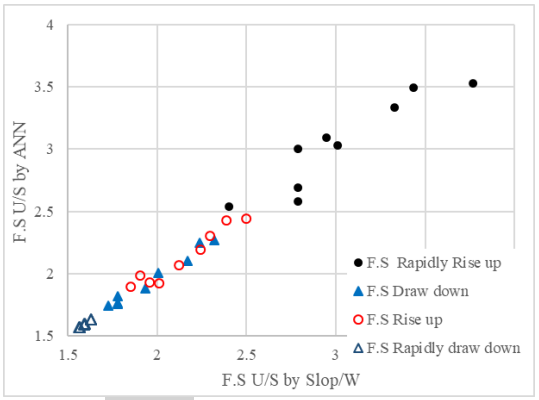

Fig 13. Model I Performance.

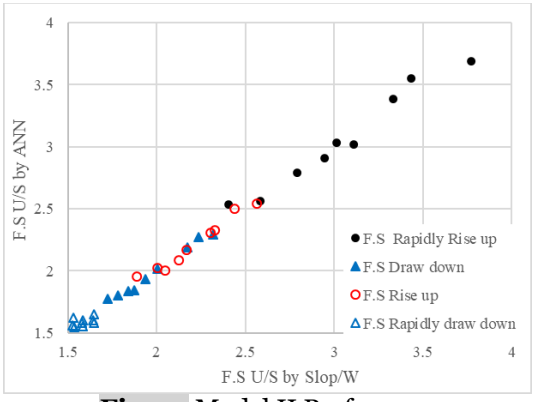

Fig 14. Model II Performance.

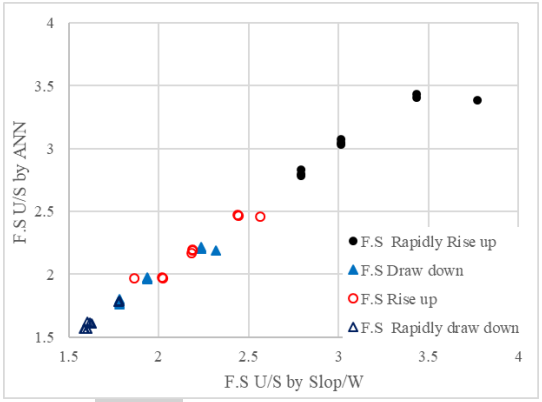

Fig 15. Model III Performance.

Table 2. Parameter Estimates

Predictor		Case Study	Predicted						
			Hidden Layer 1			Output Layer			
			H(1:1)	H(1:2)	H(1:3)	F.S Rapidly Rise up	F.S Drawdown	F.S Rise up	F.S Rapidly drawdown
Input Layer	(Bias)	I	1.130	-0.399	-0.322				
		II	-0.564	1.507	-0.250				
		III	1.298	1.152	-.013				
	kykx	I	0.408	0.034	-0.487				
		II	-1.656	-0.710	0.858				
		III	0.013	0.616	0.086				
	us	I	-2.213	-0.884	0.408				
		II	1.467	-0.498	-0.457				
		III	0.570	-.150	2.523				
Hidden Layer 1	(Bias)	I				0.141	-0.082	-0.037	0.546
		II				-1.102	-0.145	1.419	0.790
		III				-1.380	-.225	0.842	-.335
	H(1:1)	I				0.122	-0.156	0.071	-1.280
		II				-1.384	-0.812	-0.618	0.405
		III				1.817	0.539	-.299	-.961
	H(1:2)	I				-0.301	-0.847	-0.887	1.043
		II				0.742	-0.529	-1.463	-1.066
		III				-.500	-.649	-.546	0.652
	H(1:3)	I				1.243	0.755	0.749	-0.138
		II				0.214	0.987	1.058	0.157
		III				3.212	1.861	1.134	-1.686

3.3.1. Validation ANN Results

Statistical indices such as coefficient of determination (R^2), mean absolute error (MAE), average accuracy (AA), and relative error were used to evaluate the performance of the models in the present study. The qualitative comparison of model performance was categorized into four categories depending on the AA index Eq.5 [15]:

$$\begin{aligned} AA < 0.1 \quad & Excellent \text{ relation} \\ 0.1 < AA < 0.2 \quad & Good \text{ relation} \\ 0.2 < AA < 0.3 \quad & Fair \text{ relation} \\ AA > 0.3 \quad & Weak \text{ relation} \end{aligned} \quad \dots (5)$$

Table 3 displays the values involved with each of the statistical indicators associated with various models during the training and testing phase. In terms of statistical indicators related to the present study, the mean absolute error (MAE) and the coefficient (AA) were close to zero while R^2 was close to one, indicating that the outputs were accurate, and the real and predicted values were excellently related to each other. Examining these indicators for various models and flow conditions showed that the difference in model accuracy was extremely minimal and that all three models had acceptable and close responses that can be utilized throughout the test (validation) phase.

Table 3. Statistical values of ANN models

Model No.	Case Study	Coefficient of determination (R^2)	Relative Error		Mean Absolute Error (MAE)	Average Accuracy (AA)
			Training	Testing		
Model I	Rapidly Rise Up	0.997	0.009	0.0085	0.024	0.976
	Draw down	0.998	0.005	0.007	0.025	0.975
	Rise Up	0.989	0.009	0.0082	0.020	0.980
	Rapidly Draw Down	0.997	0.002	0.007	0.030	0.970
Model II	Rapidly Rise Up	0.993	0.011	0.009	0.005	0.995
	Draw down	0.989	0.009	0.0081	0.003	0.997
	Rise Up	0.995	0.013	0.0092	0.005	0.995
	Rapidly Draw Down	0.996	0.005	0.005	0.008	0.992
Model III	Rapidly Rise Up	0.996	0.004	0.004	0.013	0.987
	Draw down	0.987	0.005	0.006	0.018	0.982
	Rise Up	0.991	0.008	0.007	0.010	0.990
	Rapidly Draw Down	0.995	0.004	0.008	0.009	0.991

4.CONCLUSIONS

The following are the major outcomes of the current study; When vertical permeability was greater than horizontal permeability, results had lower values of the safety coefficient.

The presence of the core greatly contributed to enhancing the safety coefficient in the case of filling the dam reservoir by giving it the highest safety coefficient values Also, it showed the highest safety coefficient in the case of raising the water level. On the other hand, the absence of a filter affected the safety factor, which had its lowest value in all flow states.

Once the water level raised, the safety factor rapidly increased for a short period before slightly dropping to settle at a horizontal level. The initial rise in the safety factor was because the water produced a vertical pressure that stabilized and enhanced the stability of the dam service's slope. However, such behavior was the opposite of what occurred when the water level was lowered; a quick reduction in the critical safety coefficient was noticed with time, and then its value recovered.

There was a variation between the shear mobilized and the shear resistance, which tended to decrease with time when water levels rapidly rose, but the shear mobilized was never greater than the shear resistance, indicating that the model was safe under fast rising.

The accuracy of the results obtained based on the weights of the artificial neural network and the results obtained by Slope/W for models was so high.

A decrease in the safety coefficient of the downstream slope was found as a result of filling the reservoir after the end of construction.

The safety coefficient for the downstream slope differed from the condition of the steady state flow with values not exceeding 5% for the model I and model II, and less than 1% for model III for different studied cases of the flow conditions.

NOMENCLATURE

ky/kx	Hydraulic Conductivity Coefficient.
W_j	The Coefficients of Connection Weights.
R^2	Coefficient of Determination.
X_n	Normalize Value.
$\tau_{Resisting}$	Resisting Stress.
$\tau_{\text{Mobilization}}$	Mobilization Shear Strength.

REFERENCES

[1] Bakenaz A, Shahien M, Elshemy M. Seepage and Slope Stability Analysis of Earth Dams. *ICOLD*. 2018 June 1-7; Veinna.

[2] Usama R, Thair Sh. Stability Analysis of an Earth Dam Using GEOSLOPE Model under Different Soil Conditions. *Engineering and Technology Journal*. 2018; **36**(5): 523-532.

[3] Maimunah M, Kumala D. The Influence of Water Level Fluctuation Reservoir Stability of the Earth Dam. *IOP Conf. Series: Materials Science and Engineering*, 2018 December 8-9; Indonesia.

[4] Krikar M, Sirwan G . The Influence of Shell Permeability on Stability of Upstream Slope during Rapid Drawdown – Khassa

Chai Earth Dam as a Case Study. *Iraqi National Journal of Earth Sciences*. 2021; **21**(2):15-28.

[5] Saleh I, Ali M. Stability Analysis of Zoned Earth Dam under Effect of the Most Dangerous Conditions (Case Study: Khassa Chai Dam). *International Journal of Scientific & Engineering Research*. 2019; **10** (12): 110-118.

[6] Hasan T. Questioning the Parameters Used in Slope Stability Analyses of Embankment Dams. *5th Congress on Dams: Mecodonia*, 2021 September; Struga, Mecodonia.

[7] Mohammed K, Ibtisam R. Seepage and Slope Stability Analysis of Haditha Dam using Geo-Studio Software. *IOP Conf. Series: Materials Science and Engineering*, 2020 July; Thi-Qar, Iraq.

[8] Isaida B. Ivelisse Castro Martínez, Jenny García Tristá, and Yoermes González Haramboure. Influence of unsaturated soil permeability on the slopes of earth dams. *Ingeniería Hidráulica Y Ambiental*. 2019; **11**(3): 86-100.

[9] Abdolreza M, Yousef H, Farzin S, Gholam M, Gholamreza M. Performance of the horizontal drains in upstream shell of earth dams on the upstream slope stability during rapid drawdown conditions. *Arabian Journal of Geosciences*. 2014; **7**: 1957–1964.

[10] Jelena M, Milica M, Miona A, Srdjan Z, Bojan B. ANN Model for Prediction of Rockfill Dam Slope Stability. *Technical Gazette*. 2021; **2**(5):1488-1494.

[11] Erzin Y, Cetin T. The use of neural networks for the prediction of the critical factor of safety of an artificial slope subjected to earthquake forces, *Scientia Iranica*. 2012; **19**(2):188-194.

[12] Asmaa A, Muataz I. Stability and Seepage of Earth Dams with Toe Filter (Calibrated with Artificial Neural Network). *Journal of Engineering Science and Technology*. 2021; **16**(5): 3712 – 3725.

[13] Adnan J, Marewan R, Ali K. Performance Assessment of Shirin Earth Dam in Iraq Under Various Operational Conditions. *Tikrit Journal of Engineering Sciences*. 2022; **29** (2): 61-74.

[14] Kruse R., Borgelt C., Braune C., Mostaghim S., Steinbrecher M. Multilayer Perceptrons. Computational Intelligence, London; 2016.

[15] Li M, Tang X, Wu W, Liu H. General models for estimating daily global solar radiation for different solar radiation zones in mainland China. *Energy Conversion and Management*. 2013; **70**: 139-148.